

A Simple Dimeric Model Accounts for the Vibronic ECD Spectra of Chiral Polythiophenes in their Aggregated States

Daniele Padula,^[a] Fabrizio Santoro*^[b] and Gennaro Pescitelli*^[a]

^a Università di Pisa, Dipartimento di Chimica e Chimica Industriale Via G. Moruzzi 13, I-56124 Pisa, Italy

^b Consiglio Nazionale delle Ricerche – CNR, Istituto di Chimica dei Composti Organo Metallici (ICCOM-CNR), UOS di Pisa, Via G. Moruzzi 1, I-56124 Pisa, Italy

Electronic Supplementary Information

Summary

1. Theory of the vibronic model.

2. Computational Details

3. Tables

S1. TDDFT/CAM-B3LYP/SVP calculations for **Tn₂**.

S2. Calculation of Couplings with different methods for **T7₂**.

4. Figures

S1. Frontier Molecular Orbitals involved in the electronic transitions for **T7** and **T7₂**.

S2. Variation of the oscillator strength vs number of rings for **Tn**.

S3. Variation of the S0-S1 transition energies vs number of rings for **Tn**.

S4. First Effective normal mode for **Tn**.

S5-S8. Vibronic calculations including different effective modes for **Tn₂**.

S9-S12. Vibronic absorption and ECD spectra calculated for **Tn₂** as a function of the coupling potential V_{12} .

S13. Calculated vibronic spectra for **T13₂** with two different linear couplings λ_1 .

S14. Comparison between absorption and ECD spectra for PBMBT thin film and calculated for **T5₂**.

5. References

1. Theory

In this section we briefly describe our vibronic model. A more extensive illustration can be found in [1]. We consider three electronic states of the dimer, the ground state $|G\rangle$, and the two local excitations on monomer 1 and 2, $|L_1\rangle$ and $|L_2\rangle$ and adopt the following vibronic Hamiltonian

$$\mathcal{H} = |G\rangle\langle G| \mathcal{H}_G + |L_1\rangle\langle L_1| \mathcal{H}_{L_1} + |L_2\rangle\langle L_2| \mathcal{H}_{L_2} + (|L_1\rangle\langle L_2| + |L_2\rangle\langle L_1|) \mathcal{H}_{12} \quad (1)$$

where

$$\mathcal{H}_G = \mathcal{H}_1 + \mathcal{H}_2 \quad (2a)$$

$$\mathcal{H}_{L_1} = \mathcal{H}_1^* + \mathcal{H}_2 \quad (2b)$$

$$\mathcal{H}_{L_2} = \mathcal{H}_1 + \mathcal{H}_2^* \quad (2c)$$

The potential energy surface (PES) associated to the ground (\mathcal{H}_i) and excited (\mathcal{H}_i^*) Hamiltonians of monomer i are taken as harmonic and expressed as a function of the ground-state normal coordinates (\mathbf{Q}_i)

$$\mathcal{H}_i = T_i + \frac{1}{2} Q_i^T \omega_i^2 Q_i, \quad \mathcal{H}_i^* = E_i^0 + T_i + \lambda_i^T Q_i + \frac{1}{2} Q_i^T b_i Q_i \quad (3)$$

The two local excitations are coupled by \mathcal{H}_{12} and at each geometry \mathbf{Q}_i^* the eigenstates of the Hamiltonian are the adiabatic states $|G\rangle$, $|S_1\rangle$ and $|S_2\rangle$. The absorption ($\varepsilon(\omega)$) and ECD ($\Delta\varepsilon(\omega)$) spectra are computed with a time-dependent approach, by propagating the FC wavepacket on the coupled PES of $|L_1\rangle$ and $|L_2\rangle$. More specifically, saying $|G; \mathbf{0}\rangle$ the initial vibronic state (where the vector $\mathbf{0}$ specifies that it has zero quanta on each vibrational mode), the FC wavepacket obtained promoting the vibrational state of $|G; \mathbf{0}\rangle$ on either $|L_1\rangle$ or $|L_2\rangle$ are respectively $|L_1; \mathbf{0}\rangle$ and $|L_2; \mathbf{0}\rangle$. Then we have

$$\varepsilon(\omega) = \frac{4\pi N_A \times \omega}{3000 \ln(10) (4\pi\epsilon_0) \hbar c_0} \text{Re} \int_0^\infty e^{i(\omega+\omega_0)t} \left[\vec{\mu}_{L_1} \cdot \vec{\mu}_{L_1} \langle L_1; \mathbf{0} | L_2; \mathbf{0}(t) \rangle + \vec{\mu}_{L_1} \cdot \vec{\mu}_{L_2} \langle L_1; \mathbf{0} | L_2; \mathbf{0}(t) \rangle \right] dt \quad (4a)$$

$$\Delta\varepsilon(\omega) = \frac{16\pi N_A \times \omega}{3000 \ln(10) (4\pi\epsilon_0) \hbar c_0^2} \times \text{Im}[\vec{\mu}_{L_1} \cdot \vec{m}_{L_2}] \text{Re} \int_0^\infty e^{i(\omega+\omega_0)t} \langle L_1; \mathbf{0} | L_2; \mathbf{0}(t) \rangle dt \quad (4b)$$

Where $\vec{\mu}_{L_i}$ and \vec{m}_{L_i} are respectively the transition electric and magnetic dipole moment associated to monomer i . The parameters of the Hamiltonian are obtained from DFT and TD-DFT calculations adopting the CAM-B3LYP functional and the SVP basis set. The monomer PES are computed by geometry optimization and frequency analysis of the ground and first excited state. The coupling between the local excitations, as well as their

transition electric dipoles and the imaginary parts of the transition magnetic dipoles (generically denoted as \vec{d}_{Li}), are obtained by single-point TD-DFT calculations on the dimer at the C_2 equilibrium geometry of the ground state. The coupling is taken as a constant $\mathcal{H}_{12} = V_{12}$ and computed from the splitting of the energies of two-lowest excited state S_1 and S_2 , $V_{12} = (E_{S_2} - E_{S_1})/2$. Finally, the transition dipoles are obtained as linear combination of the S_1 and S_2 ones, according to the following expressions

$$\text{if } S_1 \in A \text{ and } S_2 \in B \left\{ \begin{array}{l} \vec{d}_{L1} = \frac{1}{\sqrt{2}}(\vec{d}_{S1} + \vec{d}_{S2}) \\ \vec{d}_{L2} = \frac{1}{\sqrt{2}}(\vec{d}_{S1} - \vec{d}_{S2}); \\ V_{12} < 0 \end{array} \right. ; \text{ if } S_1 \in B \text{ and } S_2 \in A \left\{ \begin{array}{l} \vec{d}_{L1} = \frac{1}{\sqrt{2}}(\vec{d}_{S1} + \vec{d}_{S2}) \\ \vec{d}_{L2} = -\frac{1}{\sqrt{2}}(\vec{d}_{S1} - \vec{d}_{S2}) \\ V_{12} > 0 \end{array} \right. \quad (5)$$

where A and B are the two irreps of the C_2 point group of symmetry.

Notice that the angles between the transition dipole moments of the local excitations are determined by the mutual orientation of the two monomers (indicated by θ in the main text). Therefore Eqs 4 show that the ECD lineshape depends on θ only through the coupling V_{12} while the ECD intensity has an additional dependence on θ due to the factor $\text{Im}[\vec{\mu}_{L1} \cdot \vec{m}_{L2}]$. On the contrary the absorption lineshape depends explicitly on θ because of the factor $\vec{\mu}_{L1} \cdot \vec{\mu}_{L2}$. This explains why the absorption lineshape is more sensitive than the ECD lineshape to the mutual orientation of the two monomers.

2. Computational Details

We obtained ground and excited states optimized geometries and harmonic analyses at (TD)DFT/CAM-B3LYP/SVP level for all \mathbf{Tn} . \mathbf{Tn}_2 geometries were generated by transforming the optimized geometry of the corresponding \mathbf{Tn} in order to obtain the desired values of r and θ . We carried out calculations of purely electronic transitions for all \mathbf{Tn} and \mathbf{Tn}_2 at TDDFT/CAM-B3LYP/SVP level. For such calculations, we used the commercial package Gaussian 09.^[2] The data obtained through harmonic analyses and electronic calculations have been used as input for our homemade codes for the generation of the effective normal modes^[3] and the computation of the quantum-dynamics of the system.^[1]

Effective modes are divided in blocks and are devised in order to reproduce the full-dimensionality vibronic spectrum of the dimer within a given resolution; the higher the required resolution the larger is the necessary number of effective modes. It was assumed that the ground and excited state of the monomer share the same normal modes and frequencies; with this approximation each block has dimension 2 and is made up by one effective oscillator per each monomer. Convergence of the spectra was checked by

increasing the number of blocks of effective modes. The evolving state was written on a product basis-set of harmonic oscillator states: the maximum allowed quantum numbers are 15, 8, 6 and 4 for the modes of the first, second third and fourth blocks, respectively. QD calculations were performed by Lanczos short iterative algorithm, computing 6 Lanczos states per propagation step (0.05 fs). In this way we obtained the correlation functions in Eqs. 4 that were Fourier transformed to obtain the spectra. Due to the adopted resolution in the frequency domain (HWHM=450 cm^{-1}) a propagation in the time interval $0 < t < 200$ fs was sufficient to obtain fully converged spectra.

3. Tables

Table S1: transition energies for the first two excited states of dimers \mathbf{Tn}_2 ($r = 5\text{\AA}$, $\theta = 15$ deg) calculated at CAM-B3LYP/SVP level. The coupling V_{12} is estimated as half the Davydov splitting, *i.e.* the S2-S1 transition energy difference.

Dimer	S1 (eV)	S2 (eV)	V_{12} (cm^{-1})
$\mathbf{T3}_2$	3.5849	3.7489	661.3
$\mathbf{T4}_2$	3.2249	3.4059	729.9
$\mathbf{T5}_2$	3.0171	3.1904	710.9
$\mathbf{T7}_2$	2.7987	2.9497	608.9
$\mathbf{T9}_2$	2.6933	2.8184	504.5
$\mathbf{T11}_2$	2.6370	2.7395	413.3
$\mathbf{T13}_2$	2.6026	2.6869	339.9

Table S2: Dependence of Coupling Potential on the angle θ for $\mathbf{T7}_2$ at $r = 5\text{\AA}$ calculated as half the Davydov splitting (TDDFT), from Mulliken Transition Charges (TrChgs) and with the Transition Density Cube (TDC) method. Transition charges and cubes of the transition densities have been obtained analyzing Gaussian 09 outputs with the freely distributed code Multiwfn (<https://multiwfn.codeplex.com/>), and the couplings have been computed with a home-made Fortran code.

θ (deg)	TDDFT (cm^{-1})	TrChgs (cm^{-1})	TDC (cm^{-1})
0	702	690	677
15	616	616	612
30	469	469	472
45	326	326	330
60	204	203	207
75	98	98	97
90	0	0	0
105	-98	-98	-97
120	-204	-203	-207
135	-326	-326	-330
150	-469	-469	-472
165	-616	-616	-612
180	-702	-690	-677

4. Figures

Figure S1: Frontier MOs involved in the first electronic transitions for **T7** (right, framed) and **T7₂** (left) calculated at CAM-B3LYP/SVP level. Horizontal black numbers are orbital energies in atomic units; vertical colored numbers are CI coefficients for the specified transition.

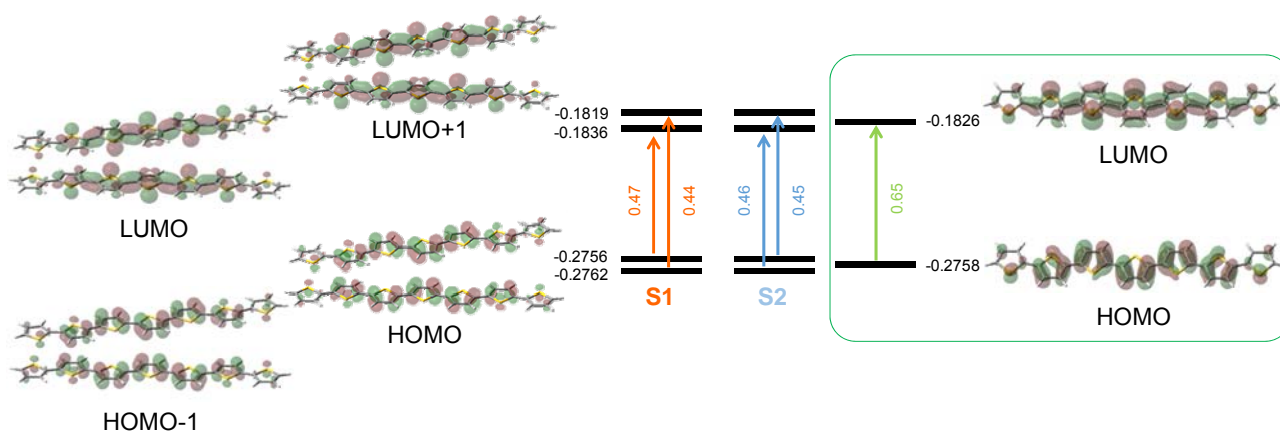


Figure S2: Oscillator strength calculated for the first excited state for **T_n** at CAM-B3LYP/SVP level as a function of **n**.

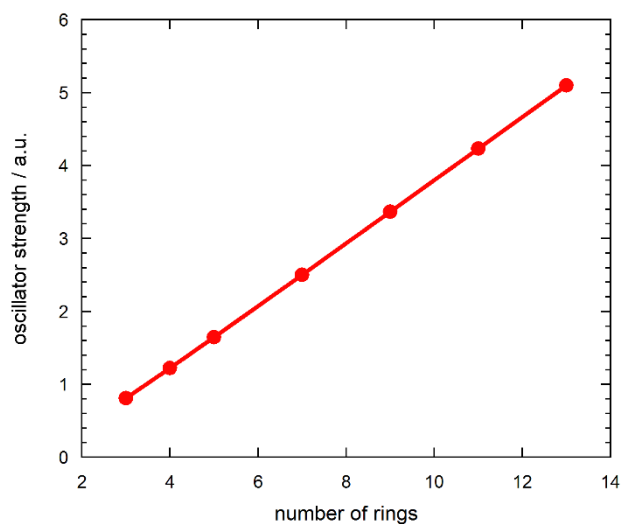


Figure S3: (a) S0-S1 transition energy in cm^{-1} calculated for **Tn** at CAM-B3LYP/SVP level as a function of **n**. (b) Same graph expressed in eV vs n^{-1} and including a fit based on W.

Kuhn's equation^[5] $E_{0-1} = a \sqrt{1 + 2b \cdot \cos\left(\frac{\pi}{n+1}\right)}$ (where both parameters *a* and *b* were fitted: $a = 5.36 \pm 0.008$, $b = -0.395 \pm 0.0004$, $R^2=0.99996$).

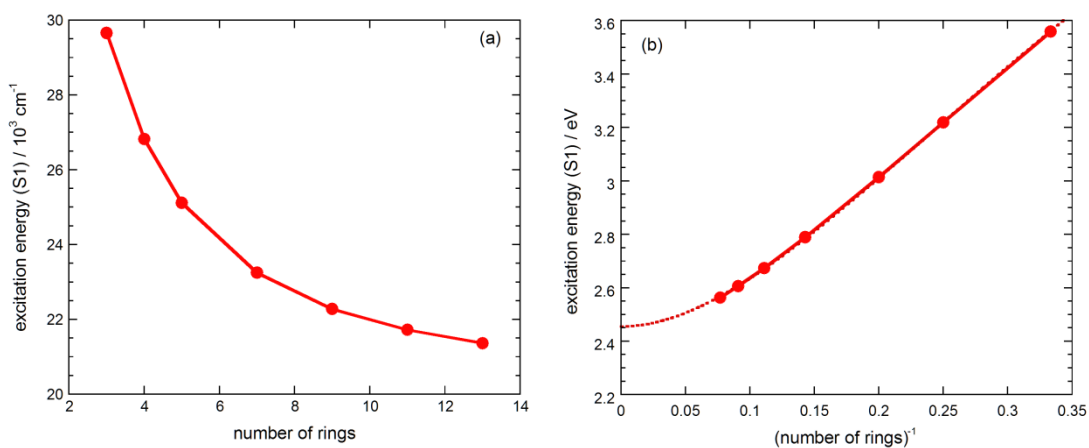


Figure S4: First effective normal mode for **T3** (top), **T5** (mid) and **T7** (bottom).

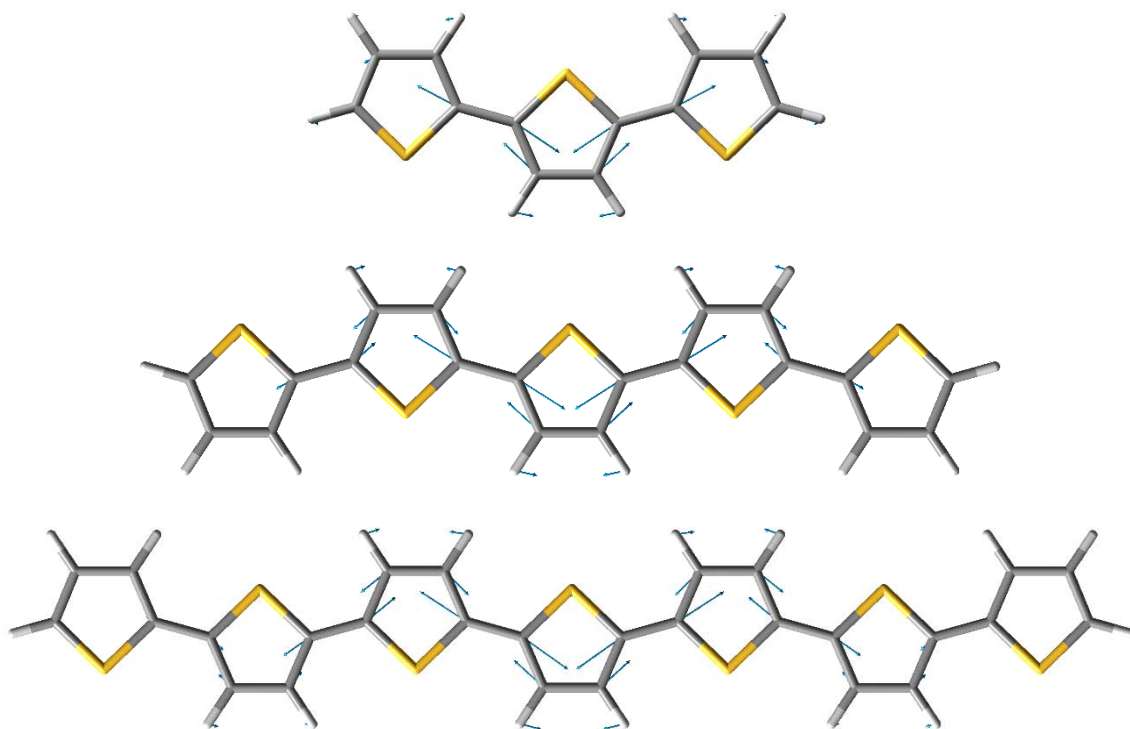


Figure S5: UV (left) and ECD (right) vibronically resolved spectra for $T3_2$ ($r = 5\text{\AA}$, $\theta = 15$ deg, HWHM = 450 cm^{-1}).

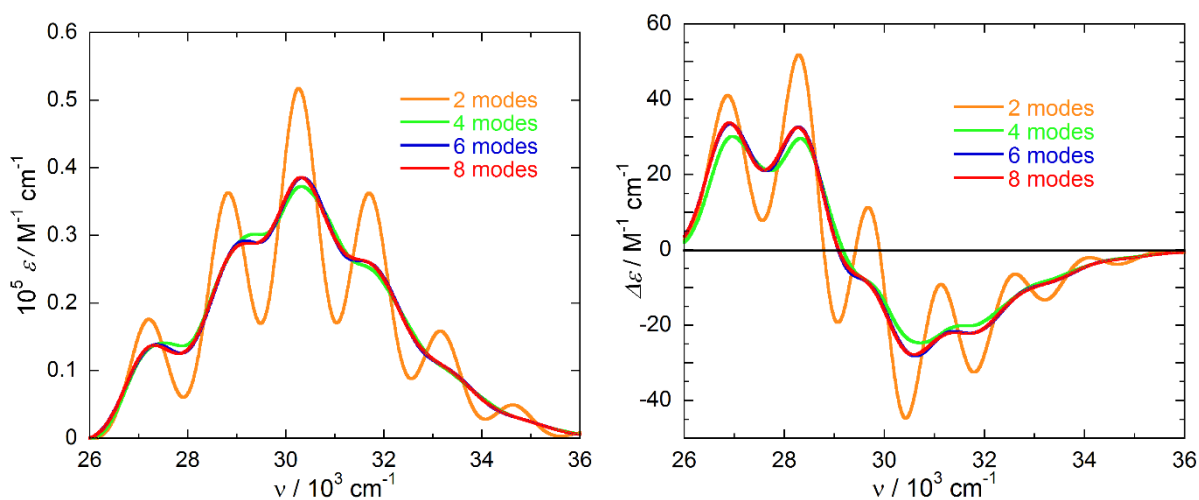


Figure S6: UV (left) and ECD (right) vibronically resolved spectra for $T4_2$ ($r = 5\text{\AA}$, $\theta = 15$ deg, HWHM = 450 cm^{-1}).

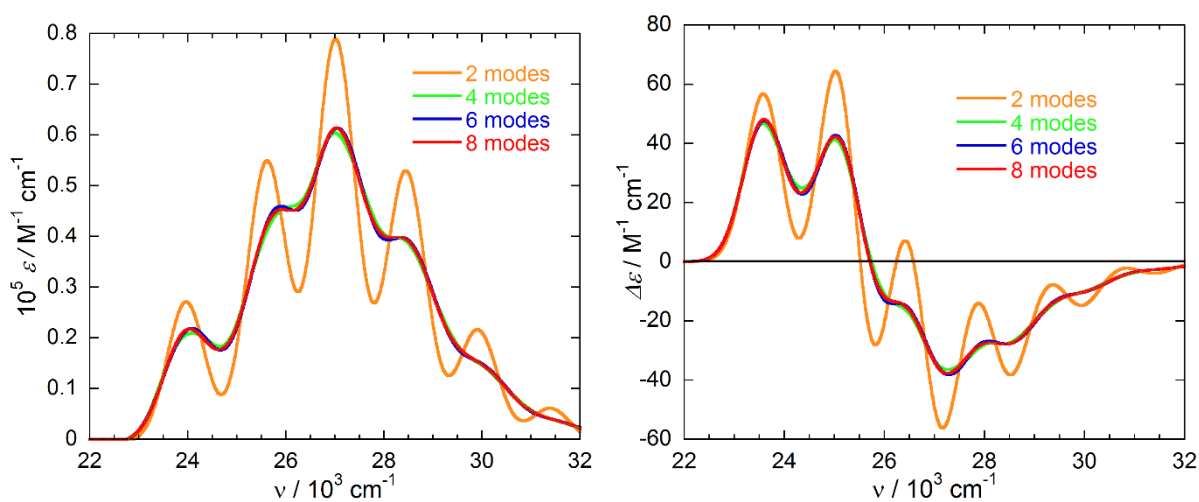


Figure S7: UV (left) and ECD (right) vibronically resolved spectra for **T5₂** ($r = 5\text{\AA}$, $\theta = 15$ deg, HWHM = 450 cm^{-1}).

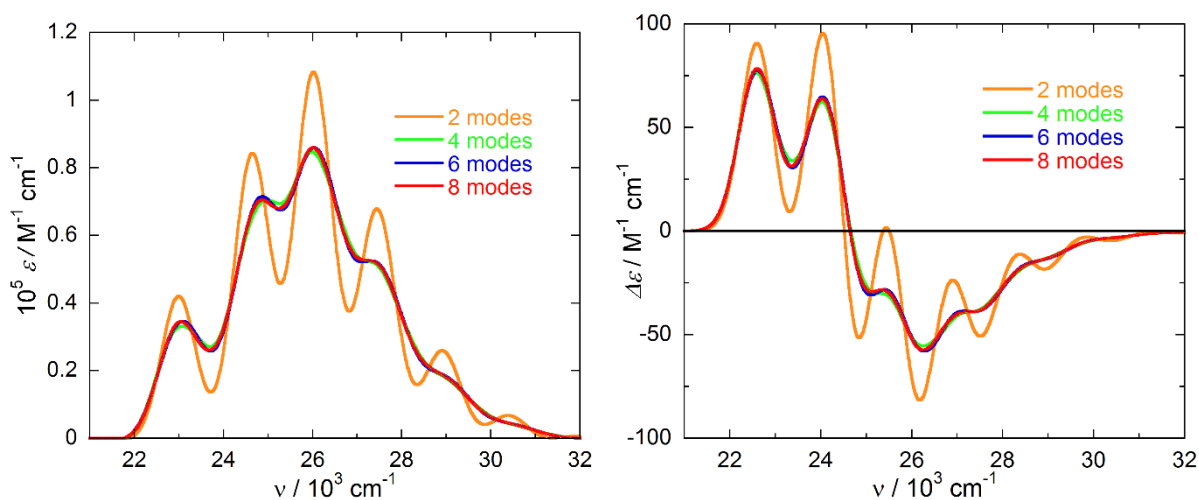


Figure S8: UV (left) and ECD (right) vibronically resolved spectra for **T7₂** ($r = 5\text{\AA}$, $\theta = 15$ deg, HWHM = 450 cm^{-1}).

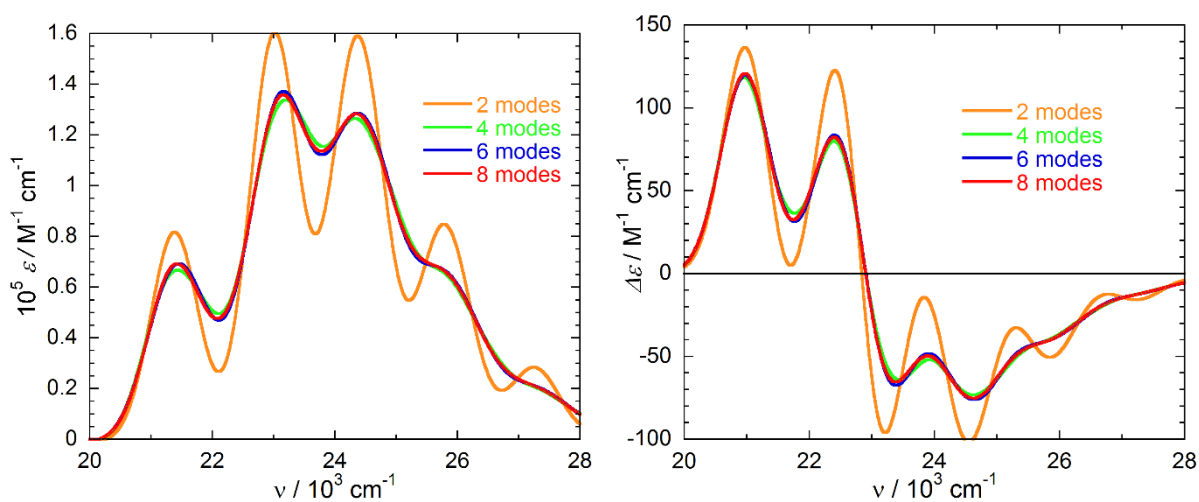


Figure S9: Calculated vibronic absorption spectra for dimer **T7₂** as a function of the coupling potentials V_{12} (given in parentheses). This latter corresponds to the indicated θ angles at a distance $r = 5 \text{ \AA}$. Spectra convoluted with HWHM = 450 cm^{-1} , 6 effective modes included. The corresponding ECD spectra are reported in the main text.

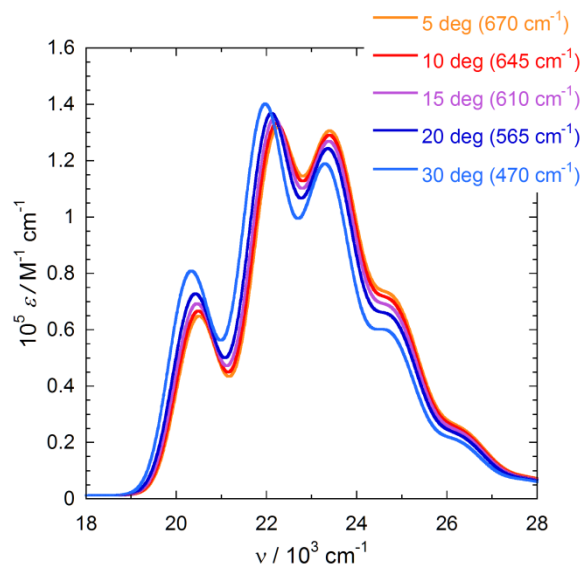


Figure S10: Calculated vibronic absorption spectra for dimer **T13₂** as a function of the coupling potentials V_{12} (given in parentheses). This latter corresponds to the indicated θ angles at a distance $r = 5 \text{ \AA}$. Spectra convoluted with HWHM = 450 cm^{-1} , 6 effective modes included. The corresponding ECD spectra are reported in the main text.

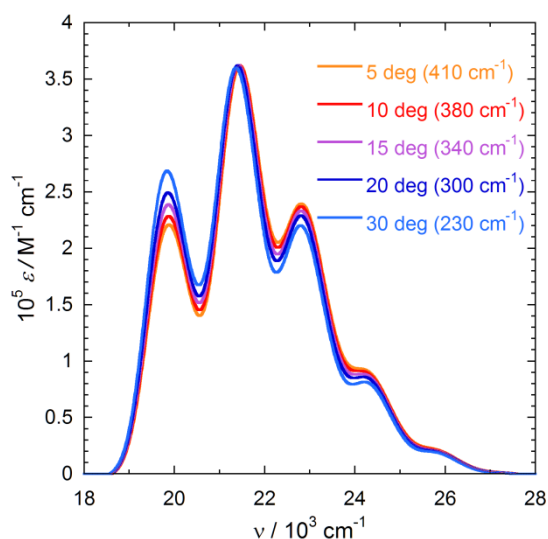


Figure S11: Calculated vibronic absorption (left) and ECD spectra (right) for dimer $\mathbf{T3}_2$ as a function of the coupling potentials V_{12} (given in parentheses). This latter corresponds to the indicated θ angles at a distance $r=5$ Å. Spectra convoluted with HWHM = 450 cm^{-1} , 6 effective modes included.

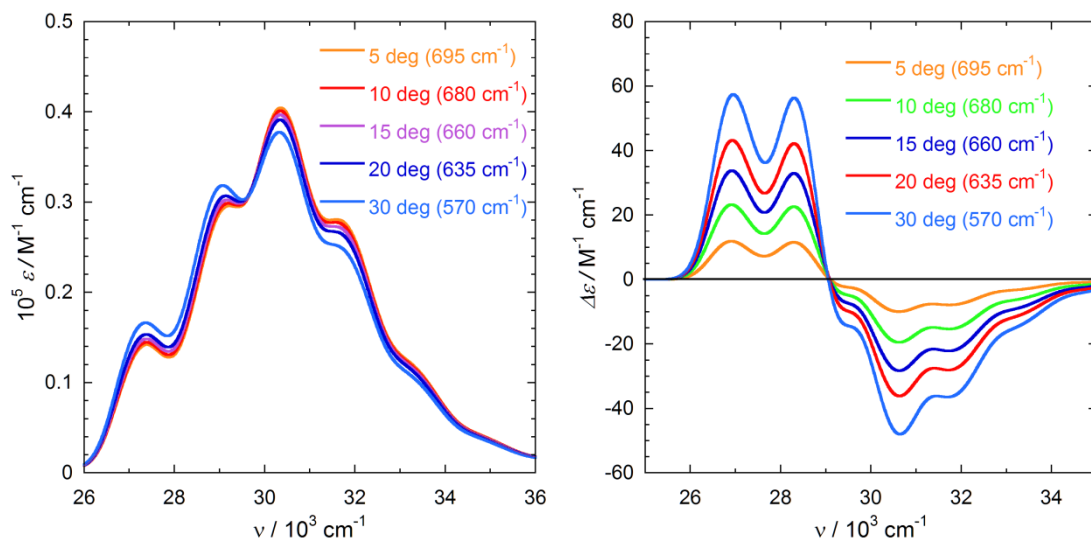


Figure S12: Calculated vibronic absorption (left) and ECD spectra (right) for dimer $\mathbf{T5}_2$ as a function of the coupling potentials V_{12} (given in parentheses). This latter corresponds to the indicated θ angles at a distance $r=5$ Å. Spectra convoluted with HWHM = 450 cm^{-1} , 6 effective modes included.

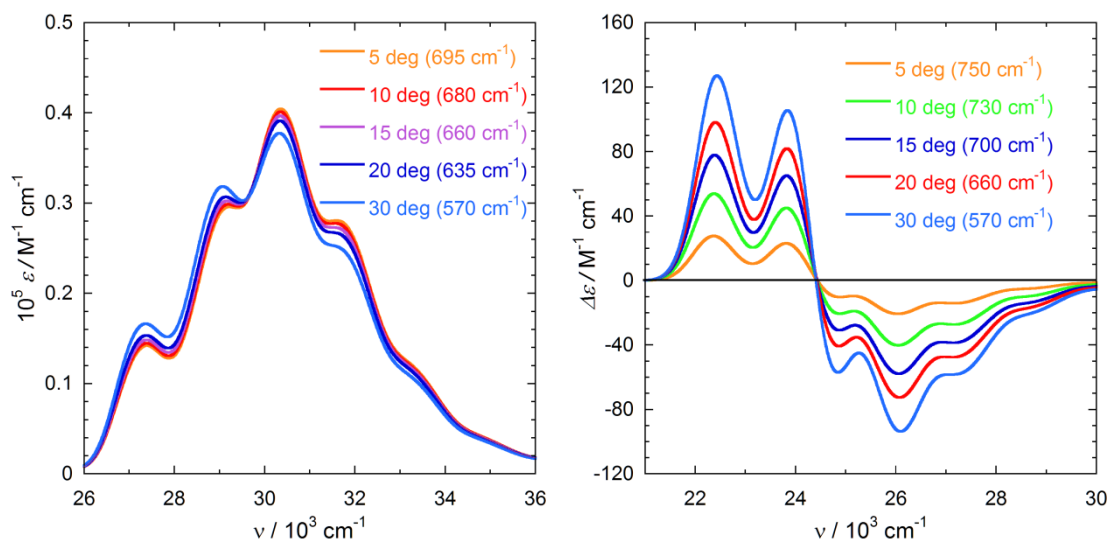


Figure S13: Calculated vibronic absorption (left) and ECD spectra (right) for dimer **T13₂** with two linear couplings λ_1 corresponding to the values calculated for **T13** (blue traces) and **T5** (red traces). In both cases $V_{12} = 340 \text{ cm}^{-1}$, corresponding $\theta = 15^\circ$ and $r = 5 \text{ \AA}$. Spectra convoluted with $\text{HWHM} = 450 \text{ cm}^{-1}$, 6 effective modes included.

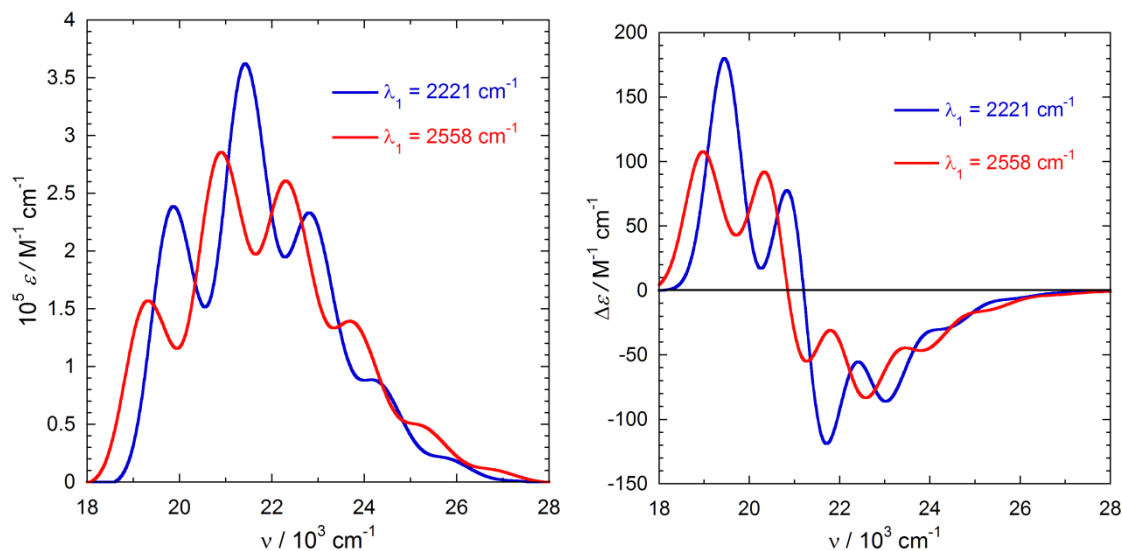
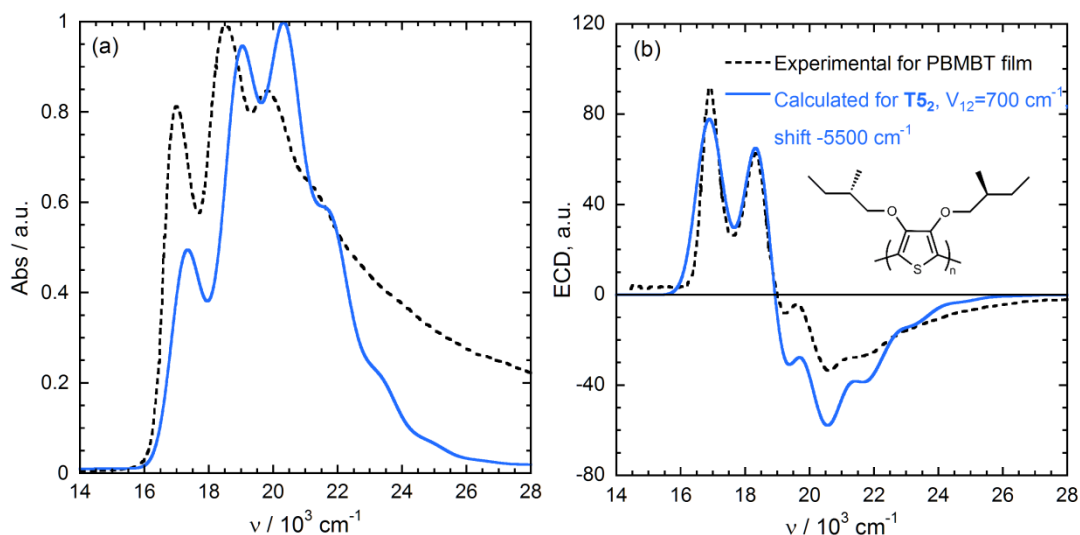


Figure S14: Comparison between experimental absorption (a) and ECD spectra (b) of PBMBT thin film, spin-cast from CHCl_3 , and calculated spectra for dimer **T5₂** with $r = 5 \text{ \AA}$ and $\theta = 15^\circ$ ($V_{12} = 700 \text{ cm}^{-1}$). Vibronic spectra convoluted with $\text{HWHM} = 450 \text{ cm}^{-1}$; 6 effective modes included; shifted by -5500 cm^{-1} . Experimental spectra reprinted from ref. [6], with permission from Elsevier. Vertical axes are ϵ and $\Delta\epsilon / \text{M}^{-1}\text{cm}^{-1}$ for the calculations, while experimental spectra (provided as OD and mdeg) were scaled arbitrarily.



5. References

- [1] D. Padula, D. Picconi, A. Lami, G. Pescitelli, F. Santoro, *J. Phys. Chem. A* **2013**, *117*, 3355-3368.
- [2] Gaussian 09, Revision D.01. M. J. Frisch, G. W. Trucks, H. B. Schlegel, G. E. Scuseria, M. A. Robb, J. R. Cheeseman, G. Scalmani, V. Barone, B. Mennucci, G. A. Petersson, H. Nakatsuji, M. Caricato, X. Li, H. P. Hratchian, A. F. Izmaylov, J. Bloino, G. Zheng, J. L. Sonnenberg, M. Hada, M. Ehara, K. Toyota, R. Fukuda, J. Hasegawa, M. Ishida, T. Nakajima, Y. Honda, O. Kitao, H. Nakai, T. Vreven, J. Montgomery, J. A., J. E. Peralta, F. Ogliaro, M. Bearpark, J. J. Heyd, E. Brothers, K. N. Kudin, V. N. Staroverov, R. Kobayashi, J. Normand, K. Raghavachari, A. Rendell, J. C. Burant, S. S. Iyengar, J. Tomasi, M. Cossi, N. Rega, J. M. Millam, M. Klene, J. E. Knox, J. B. Cross, V. Bakken, C. Adamo, J. Jaramillo, R. Gomperts, R. E. Stratmann, O. Yazyev, A. J. Austin, R. Cammi, C. Pomelli, J. W. Ochterski, R. L. Martin, K. Morokuma, V. G. Zakrzewski, G. A. Voth, P. Salvador, J. J. Dannenberg, S. Dapprich, A. D. Daniels, O. Farkas, J. B. Foresman, J. V. Ortiz, J. Cioslowski, D. J. Fox. Wallingford CT, 2013.
- [3] D. Picconi, A. Lami, F. Santoro, *J Chem Phys* **2012**, *136*, 244104.
- [4] B. M. W. Langeveld-Voss, R. A. J. Janssen, E. W. Meijer, *J. Mol. Struct.* **2000**, *521*, 285-301.
- [5] W. Kuhn, *Helv. Chim. Acta* **1948**, *31*, 1780–1799.
- [6] B. M. W. Langeveld-Voss, R. A. J. Janssen and E. W. Meijer, *J. Mol. Struct.*, **2000**, *521*, 285-301.